Atmospheric circulation as a factor contributing to increasing drought severity in Central Europe

Preprint · January 2020

DOI: 10.13140/RG.2.2.19313.84322

6 authors, including:

Ondřej Lhotka
The Czech Academy of Sciences
15 PUBLICATIONS **221** CITATIONS
SEE PROFILE

Jan Kyselý
Institute of Atmospheric Physics, Czech Academy of Sciences
163 PUBLICATIONS **4,817** CITATIONS
SEE PROFILE

Yannis Markonis
Czech University of Life Sciences Prague
70 PUBLICATIONS **549** CITATIONS
SEE PROFILE

Jan Balek
Czech Globe
52 PUBLICATIONS **1,035** CITATIONS
SEE PROFILE

Atmospheric circulation as a factor contributing to increasing drought severity in Central Europe

Ondřej Lhotka[1,2], Mirek Trnka[2], Jan Kyselý[1,3], Yannis Markonis[3], Jan Balek[2], Martin Možný[2,4]

[1]Institute of Atmospheric Physics of the Czech Academy of Sciences, Prague, Czech Republic

[2]Global Change Research Institute of the Czech Academy of Sciences, Brno, Czech Republic

[3]Faculty of Environmental Sciences, Czech University of Life Sciences, Prague, Czech Republic

[4]Czech Hydrometeorological Institute, Prague, Czech Republic

Corresponding author: Ondřej Lhotka (ondrej.lhotka@ufa.cas.cz)

Key Points:

- Dryness of the 2015–2018 period was record-breaking in Central Europe according to the Palmer Drought Severity Index
- Statistically significant trends toward drier condition were found for long-term drought indices
- Increased drought severity in the past decades was linked to higher frequency of dry circulation types at the expense of wet types

Abstract

Long-lasting and severe droughts seriously threaten agriculture, ecosystems, and society. Summer 2018 in Central Europe was characterized by unusually persistent heat and drought, causing substantial economic losses, and became a part of a several years long dry period observed across this region. This study assesses the magnitude of recent drought within a long-term context and links the increased drought severity to changes in atmospheric circulation. Temporal variability of drought conditions since the late 19th century was analyzed at 7 long-term stations distributed across the Czech Republic using the Palmer Drought Severity Index and the Standardized Precipitation Evaporation Index. The Palmer Z-Index and a variation of the Standardized Precipitation Evaporation Index were used to study rapidly emerging short-term droughts and to link these episodes to atmospheric circulation. Changes in circulation were analyzed through circulation types calculated from circulation indices (flow strength, direction and vorticity) using mean sea level pressure data from the NCEP/NCAR reanalysis for 1948 to the present. Increased drought severity across the Czech Republic with record-low values during 2013–2018 occurred at most stations. This was distinctive in both vegetation (April–September) and cold (October–March) periods. The tendency to more severe droughts in recent decades was linked to changes in frequency of dry and wet circulation types, highlighting the important role of atmospheric circulation in regional climate. It remains open whether the significantly increasing frequency of dry circulation types in the vegetation period is related to climate change, or rather represents multi-decadal climate variability.

1 Introduction

Drought is a complex hazard that is dangerous through its insidious onset and large spatial extent (Spinoni et al., 2017). It is usually associated with substantial economic losses especially in agriculture (Ding et al., 2011), which are often regarded as a precursor of famine and conflicts in the rapidly growing population of the developing world (UN, 2018). Although impacts of individual drought events on global crop productivity are difficult to prove, a recent study by Trnka et al. (2019) showed a link between the size of drought-affected areas and global wheat and cereal prices. Many drought indices relying on various data and methods have been developed in order to analyze duration and severity of droughts, ranging from the relatively simple Standardised Precipitation Index (SPI; Guttman, 1998) to advanced satellite- and model-based indices (WMO & GWP, 2016). The most important advantages of SPI are its relatively easy calculation, usage, and feasible applicability in various climate zones. Therefore, the WMO has recommended SPI as the main meteorological drought index that countries should use to monitor drought conditions (Hayes, 2011).

It should be noted, however, that the absence of a temperature component in SPI limits its applicability in the warming climate, with its higher potential evapotranspiration. The compound nature of drought is better captured by indices considering changes in evapotranspiration, such as the Palmer Drought Severity Index (PDSI; Palmer, 1965) or Standardized Precipitation Evaporation Index (SPEI; Vicente-Serrano et al., 2010). Sheffield et al. (2012) showed that PDSI values depend on different methods for estimating potential evapotranspiration. Use of the physically based Penman–Monteith algorithm (Allen et al., 1998) resulted in less severe drought conditions compared to the Thornthwaite (1948) approach, which is based solely on temperature. This behavior has been especially evident since the 1980s (Sheffield et al., 2012), when a relatively rapid increase in global temperature was observed (Hartmann et al., 2013).

By contrast, Dai (2011) concluded that use of the Penman–Monteith algorithm only slightly reduces the drying trend seen in PDSI with the basic Thornthwaite model and showed increased aridity since 1950 over many land areas, especially in Africa and Southeastern Asia but also in Europe. Dai (2011) also demonstrated that the majority of this drying was due to temperature increases. In Europe, drought patterns varied over regions analyzed but a small, continuous increase of the European areas prone to drought from the early 1980s onwards was found (Spinoni et al., 2015). The authors showed that during the 1950–2012 period Northern and Eastern Europe exhibited the largest drought frequency and severity from the 1950s to 1970s, while Western and Southern Europe (especially the Mediterranean) were struck by major droughts from the 1990s to 2010s. Increasing drought tendency in the Iberian Peninsula over recent decades was shown also by Vicente-Serrano et al. (2015), who linked this phenomenon to a greater atmospheric evaporative demand associated with temperature rise. These drier conditions over the Mediterranean are in accordance with a recent north–south polarization of drought patterns over Europe (Markonnis et al., 2018).

The current study focuses on the Czech Republic, in which the shift to drier conditions is also evident. Trnka et al. (2009) found negative trends in PDSI in this region since the 1940s especially for the growing season (April–September) and linked them to the increased frequency of warm and dry "southerly", "easterly" and "high-pressure system over Central Europe" Hess–Brezowsky circulation types (Werner & Gerstengarbe, 2009). These findings are in accordance with Brázdil et al. (2015), who studied drought episodes in the 1805–2012 period using the SPEI and PDSI indices and concluded that while dry episodes in the 19th century can be attributed mainly to below-average precipitation, the most recent droughts were associated rather with the increase in temperatures. Both aforementioned studies used the Thornthwaite approach for estimating moisture supply and demand. The more detailed analyses of droughts between 1961 and 2012 showed clear decrease of soil moisture content in the top soil layer (1 m depth), using observed and modelled time series across the Czech Republic (Trnka et al., 2015). The results are in accordance with more negative PDSI values observed in the past two decades (Brázdil et al., 2015; Trnka et al., 2009) and support suitability of the Thornthwaite method for analyzing changes in drought patterns in the Czech Republic.

Across this region, the summer of 2015 was very hot and dry (Hoy et al., 2017; Ionita et al., 2017; Lhotka et al., 2018b) and this drier period persisted for three more years, peaking in summer 2018, when substantial crop failures were reported along with major economic losses (EC, 2018). There are concerns whether this drying trend will continue or even accelerate due to projected increase of global temperature (Collins et al., 2013) and more intense and longer lasting heat waves (Fischer et al. 2010; Lhotka et al. 2018a), during which the evaporative demand is considerably larger (Miralles et al., 2014; Stéfanon et al., 2014). The main aims of the study are to analyze severity of the Central European 2015–2018 drought event in the long-term context (since the end of the 19th century) and study its links to atmospheric circulation. The search for drivers of drought continues to influence societal discourse in many parts of Europe, and analysis of the underlying causes is highly relevant for such debate.

2 Data and Methods

2.1 Drought indices

The severity of droughts was assessed for 7 long-term stations located in the Czech Republic, their elevations ranging roughly from 200 to 450 m a.s.l. (Figure 1a). The sites

represent weather stations with the longest daily precipitation and temperature records available within the Czech Hydrometeorological Institute database. The study applies four drought indices (Table 1). Palmer Drought Severity Index (PDSI; Palmer, 1965) was one of the first historical attempts to identify droughts using more than just precipitation data. This index incorporates precipitation, temperature, and water-holding capacity of soils. Although it originally was developed to identify droughts affecting agriculture, PDSI is used today also for other applications. Palmer Z Index (PZIN) is a first step in estimating PDSI and it expresses anomaly in water balance over the calculation period. It therefore responds to short-term conditions better than does PDSI and enables identifying rapidly developing drought conditions (WMO and GWP, 2016). Another drought index applied is the Standardized Precipitation Evaporation Index (SPEI; Vicente-Serrano et al., 2010) that uses precipitation and temperature data only. Two versions of SPEI were calculated: SPEI-52, which characterizes rather long-term droughts, and SPEI-4, which is more suitable for analyzing short-term events. All drought indices were calculated using temperature and precipitation data only, because other drought-related meteorological variables (e.g., solar radiation, wind speed, and humidity) are not available in these historical records. The indices are available in weekly temporal resolution (52 values per year) from the start of the individual stations' observation to 2018. The longest records are available for Prague-Klementinum and Tabor (1876–2018, 143 years) while the shortest series at Klatovy starts in 1922 (97 years).

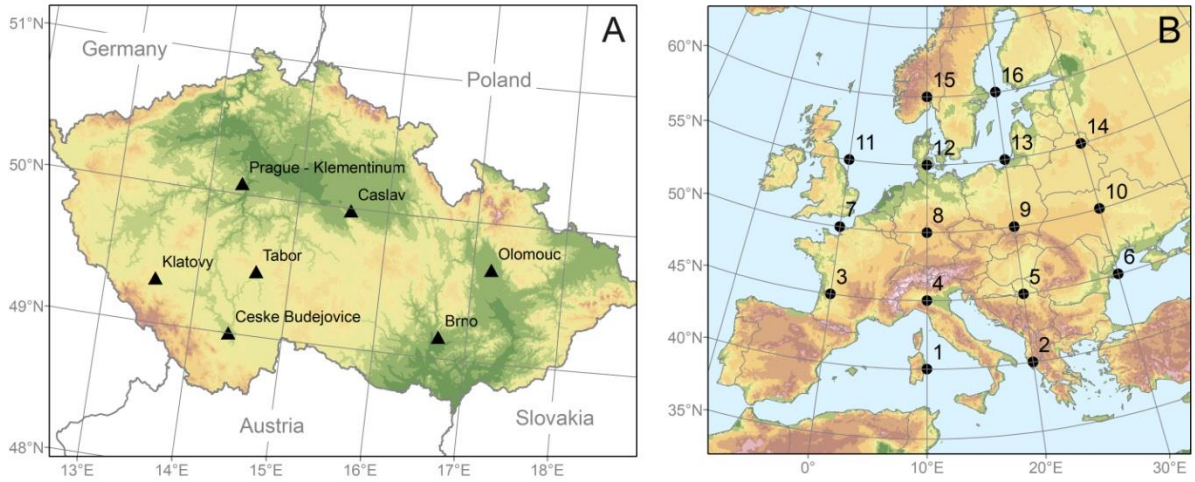

Figure 1. (A) Locations of stations used and (B) points for circulation indices' calculation.

Table 1

Drought indices used

Drought index	Abbreviation	Input variables	Characteristic
Palmer Drought Severity Index	PDSI	P, T, AWC	long-term
Palmer Z Index	PZIN	P, T, AWC	short-term
Standardized Precipitation Evaporation Index (52 weeks)	SPEI-52	P, T	long-term
Standardized Precipitation Evaporation Index (4 weeks)	SPEI-4	P, T	short-term

P – precipitation, T – temperature, AWC – available water content

The individual drought indices respond differently to changes in input variables. Distributions of weekly changes in drought indices (hereafter referred to as tendencies) are shown in Figure 2 (example for Prague, the results are analogous for the other stations). The tendencies were calculated separately for the vegetation period (VEG, weeks 14–39, roughly April–September) and the cold period (COLD, weeks 40–13, approximately October–March). There were significant differences between VEG and COLD in the shapes of their distributions (according to Kolmogorov–Smirnov test at the 5% level), except for SPEI-4. The PDSI, PZIN, and SPEI-52 indices had lower kurtosis in VEG compared to COLD and, in addition, PDSI was positively skewed in both seasons (Figure 2). As expected, the short-term drought indices (PZIN and SPEI-4) exhibited larger values of weekly tendencies compared to the long-term ones and thus they are more suitable for linking drought to changes in atmospheric circulation.

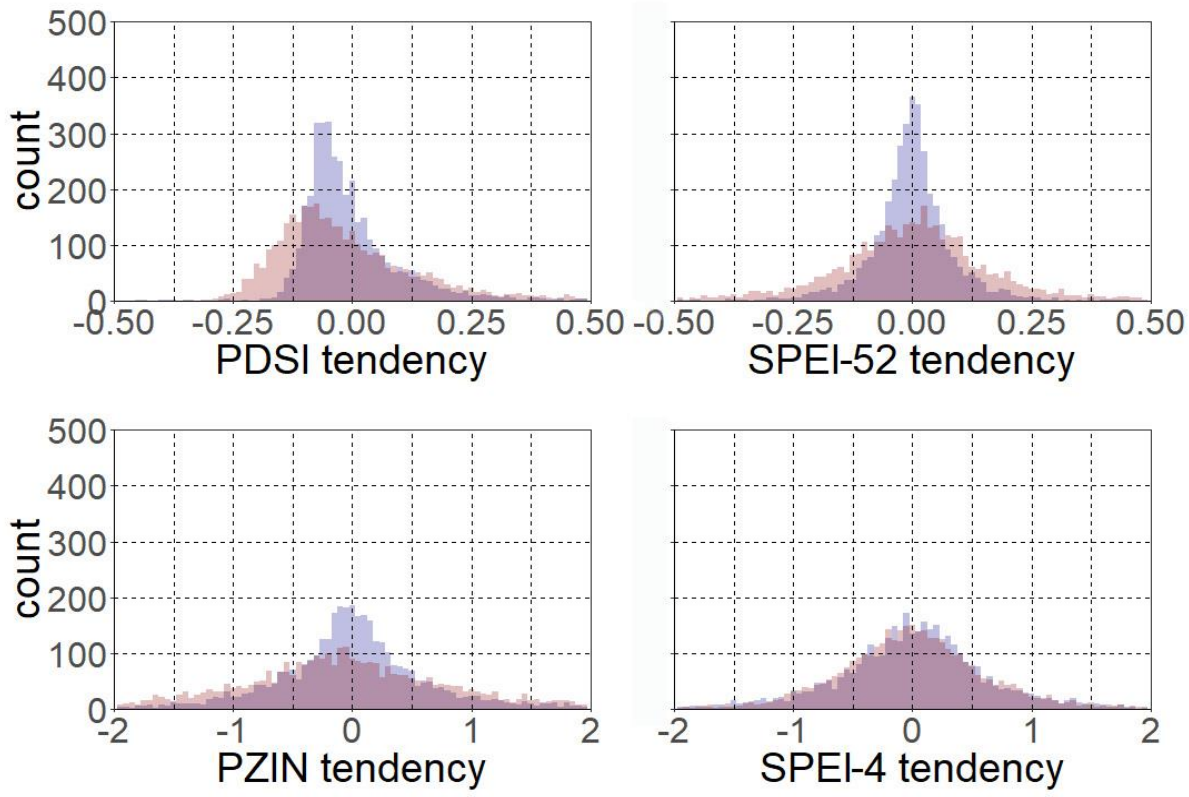

Figure 2. Distributions of weekly changes (tendencies) in the drought indices for Prague-Klementinum considering the vegetation (red) and cold (blue) periods. Drought indices' abbreviations are listed in Table 1.

2.2 Circulation indices and types

Atmospheric circulation over Central Europe was characterized by circulation types derived from circulation indices. The indices (flow strength, direction, and vorticity; Jenkinson and Collison, 1977; Plavcová & Kyselý, 2011) were calculated at the daily timescale using sea level pressure at 16 points regularly distributed across Europe, centered at 50°N and 15°E (Figure 1b). The sea level pressure data was taken from the NCEP/NCAR reanalysis (Kalnay et al., 1996), which is available from 1948 onward. The first circulation index is a flow strength (STR), which is a vector sum of western (w) and southern flow (s) components:

$$w = 0.5 \times (P4 + P5) - 0.5(P12 + P13)$$

$$s = 1.56 \times (P13 + 2 \times P9 + P5) - 0.25 \times (P12 + 2 \times P8 + P4)$$

$$STR = w + s$$

where P(1–16) indicate sea level pressure value for a given point in hPa. The second circulation index, flow direction (DIR), is calculated using a multi-valued inverse tangent function and is given by the formula:

$$DIR = atan2(w, s)$$

The third circulation index is flow vorticity (VORT), which is the sum of its zonal (zw) and meridional (zs) components and reflects the rotation of an air mass. It indicates anticyclonic (VORT < 0) or cyclonic (VORT > 0) weather conditions and is calculated using the formulas:

$$zw = 1.08 \times [0.5 \times (P1 + P2) - 0.5 \times (P8 + P9)] - 0.94 \times [0.5 \times (P8 + P9) - 0.5 \times (P15 + P16)]$$

$$zs = 1.21 \times [0.25 \times (P14 + 2 \times P10 + P6) - 0.25 \times (P13 + 2 \times P9 + P5) - 0.25 \times (P12 + 2 \times P8 + P4) + 0.25 \times (P11 + 2 \times P7 + P3)]$$

$$VORT = zw + zs$$

In the next step, 27 circulation types were derived from the STR, DIR, and VORT indices (similarly to Plavcová & Kyselý, 2011). If STR and VORT values were lower than 4, the pressure field lacked distinctive features and that day was left unclassified (U). When the absolute value of VORT is at least five times larger than STR, strongly anticyclonic (A, if VORT < 0) or strongly cyclonic (C, if VORT > 0) type was assigned. If STR was larger than the absolute value of VORT, the day was classified into one of the eight directional circulation types (N, NE, E, SE, S, SW, W, NW). The remaining days were assigned to hybrid circulation types based on their direction and anticyclonic or cyclonic vorticity (e.g., ASW, CW).

Frequencies of individual circulation types in VEG and COLD are shown in Figure 3. Overall, strongly cyclonic and hybrid cyclonic circulation types were less abundant compared to their anticyclonic analogues and directional circulation types during both seasons. For VEG, the largest frequency was found for the A type (7.2%), while AW, ANW, W, and U all had frequencies larger than 5%. In COLD, by contrast, advection from the western quadrant dominates, and ASW, AW, SW, and W circulation types accounted for more than one-third of days in the 1948–2018 period. The pressure field in COLD tended to be more distinctive, and therefore the U circulation type appeared far less frequently in COLD compared to VEG (cf. 1.1% vs. 5.3%, Figure 3).

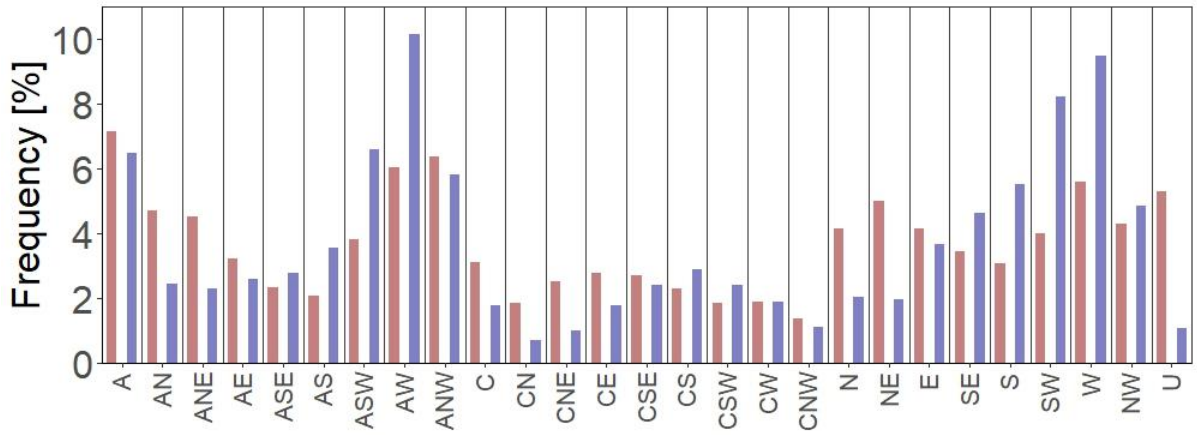

Figure 3. Frequencies of individual circulation types over Central Europe for the vegetation (red) and cold (blue) periods over 1948–2018.

2.3 Linking drought indices to atmospheric circulation

Relationships between droughts and atmospheric circulation were studied through weekly tendencies of short-term drought indices (PZIN and SPEI-4), which have larger signal-to-noise ratios due to the larger changes between individual weeks (Figure 2). A negative tendency suggests drier conditions compared to the previous week and vice versa. PZIN and SPEI-4 indices were averaged across all seven stations. Using actual drought values would not be straightforward due to a relatively long soil moisture memory (Delwarth & Manabe, 1988). The drought tendencies in weekly resolution, however, cannot simply be linked to more dynamically changing daily circulation types (Supplementary Table 1). In order to overcome this issue, as many as seven daily circulation types were assigned to one weekly drought tendency value. When only one circulation type was classified during the given week (which happens rather rarely), it received a weight of 7. Analogously if two or more circulation types occurred in the given week, they were given weights between 1 and 6 according to their duration in days within that week. For each circulation type a weighted average was calculated for COLD and VEG in order to analyze its conduciveness to drought.

3 Results

3.1 Temporal variability of drought events

Using PDSI calculated for seven stations across the Czech Republic, long-term temporal variability of drought events was analyzed (Figure 4). The most distinctive feature recorded at all stations was the presence of extreme droughts (PDSI value lower than –4) from the 2000s onward. PDSI dropped below –6 in 2018 at stations Brno and Prague, demonstrating drought conditions unprecedented since the late 19th century (Figure 4a,f). In Prague, extreme drought was observed from summer 2015 onward (for more than 3 years), creating the longest consecutive extreme drought event. Extreme drought episodes were recorded also prior to the 2000s, but these were not spatially coherent, for example around 1945 in Klatovy and during 1985 in Ceske Budejovice.

All stations had negative PDSI trends (considering their whole periods of observation) ranging from –0.13 to –0.38 per decade, and similar trend values were found in the overlapping

1922–2018 period (Table 2). All trends were significant at the 5% level according to the modified Mann–Kendall trend test for autocorrelated data (Yue & Wang, 2004). Larger differences in PDSI trends were observed during 1948–2018, a period covered by the NCEP/NCAR reanalysis that provides sea level pressure data for assessing atmospheric circulation. The most pronounced PDSI trends were found in Brno and Prague (–0.54/decade), while the trend was close to zero in Ceske Budejovice due to severe droughts in the 1950s and 1980s (Figure. 4c). The most recent 1979–2018 period (its onset corresponding with the beginning of satellite measurements) was characterized by the largest negative PDSI trends (especially in Brno, Caslav, and Prague; Table 2). Analogously to the earlier period, an indistinct statistically insignificant trend was observed in Ceske Budejovice, mainly due to the 1980s extreme drought.

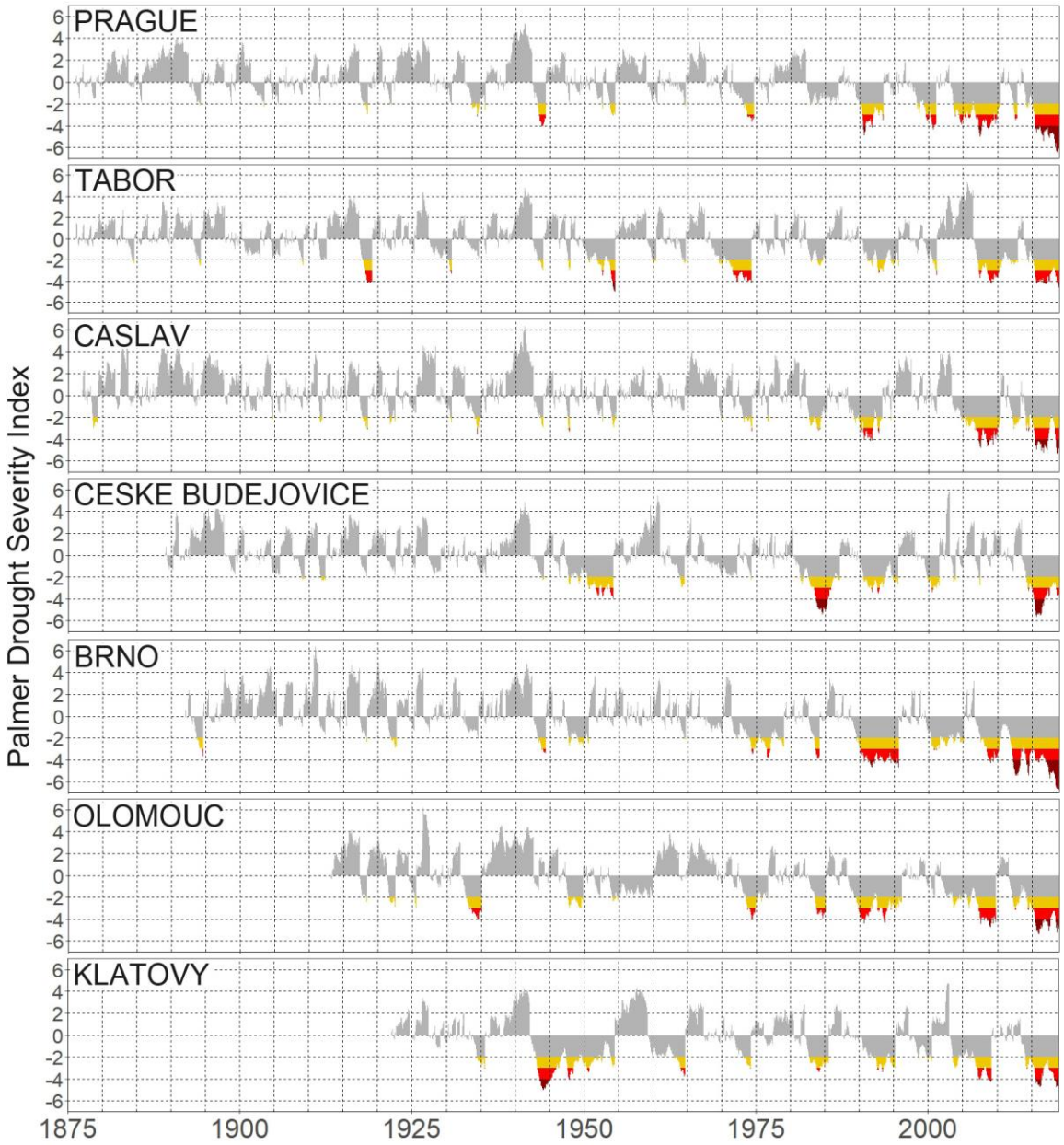

Figure 4. Temporal variability of Palmer Drought Severity Index at 7 stations analyzed. Yellow color indicates moderate, red severe, and dark red extreme drought conditions.

Table 2

Linear trends of the Palmer Drought Severity index per decade for 7 stations analyzed (sorted by length of available data), considering four different time periods.

Station	Start year of data	Trend (whole period)	Trend (1922–2018)	Trend (1948–2018)	Trend (1979–2018)
Prague	1876	–0.28*	–0.44*	–0.54*	–0.96*
Tabor	1876	–0.13*	–0.21*	–0.16	–0.63*
Caslav	1877	–0.20*	–0.32*	–0.43*	–0.81*
Ceske Budejovice	1889	–0.18*	–0.17*	–0.08	+0.09
Brno	1892	–0.35*	–0.44*	–0.54*	–0.97*
Olomouc	1913	–0.38*	–0.38*	–0.40*	–0.65*
Klatovy	1922	–0.19*	–0.19*	–0.22*	–0.59*

*Denotes trends statistically significant at the 5% level

In the next step, we analyzed drought episodes in more detail in COLD and VEG. The time series were averaged for all seven stations, and therefore the limited overlapping 1922–2018 period was studied. Considering PDSI, the 2015–2018 period had by far the lowest values in both seasons analyzed (with a minimum of –4.5 in COLD during 2015/16 and the same value was found in VEG during 2018, Figure 5). This period fell outside the confidence interval defined as the mean PDSI ± 2 × standard deviation for 1922–1999. PDSI values below this interval were recorded also in 1991 and 2007 for VEG and during 1998/99 for COLD. Confidence intervals were calculated analogously for the other drought indices.

A similar pattern was found considering another long-term index, SPEI-52. The last four years of observation were extremely dry especially in VEG, but a record-breaking SPEI-52 value (–2.3) was found for COLD in 2015/16. During VEG, the record-breaking SPEI-52 value (–1.8) occurred in 2007 but the 2018 season ranked as the second driest. In general, the PDSI and SPEI-52 indices showed similar temporal variability patterns for COLD and VEG, mainly due to their long-term nature.

Differences between seasons are more pronounced for short-term indices. The driest COLD was recorded in 1953/54, with the PZIN value of –0.7 and SPEI-4 value of –1.0. Only two other years fell outside the confidence interval in this season (2006/07, and 2013/14), and there was good agreement between PZIN and SPEI-4. During VEG, short-term indices revealed rapidly emerging droughts in 1947, 2015, and 2018. These three seasons were linked to the three lowest values of both PZIN and SPEI-4. The long-term (PDSI and SPEI-52) indices showed statistically significant negative trends for both seasons (using Mann–Kendall trend test at the 5% level), which was associated with the extremely dry recent 2015–2018 period (Figure 5). Considering short-term indices, however, statistical significance was determined for PZIN in VEG only.

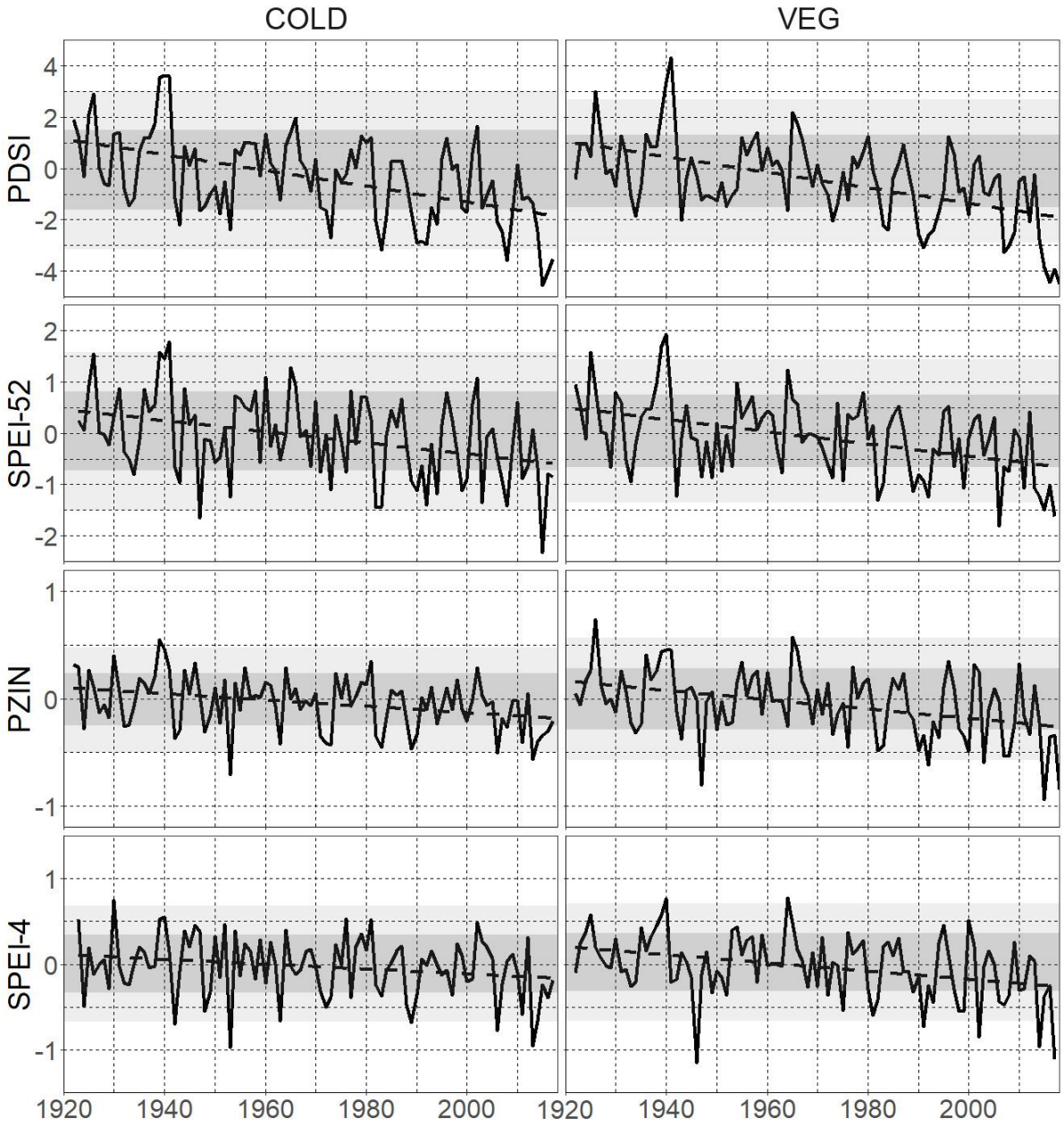

Figure 5. Temporal variability of drought indices during October–March (COLD) and April–September (VEG) seasons. The time series (1922–2018) were created by averaging drought indices from the 7 stations shown in Figure 1a. On the x-axis, labels indicate the beginning of cold seasons spanning parts of two calendar years (e.g., 2000 indicates the 2000/01 cold season).

3.2 Links to atmospheric circulation

Relationships between drought episodes and 27 circulation types were analyzed for the 1948–2018 period, for which sea level pressure data from the NCEP/NCAR reanalysis were available. These circulation types were linked to drought tendencies (Section 2.3) using short-term PZIN and SPEI-4 indices. Figure 6 shows mean drought tendency for each circulation type in COLD and VEG, where negative tendencies suggest increase of dry conditions and positive tendencies correspond to moister regime. The anticyclonic circulation types had negative mean drought tendencies (down to –0.29 considering PZIN and –0.15 for SPEI-4). By contrast, all cyclonic circulation types were related to positive mean drought tendencies and their magnitudes were larger compared to those under anticyclonic circulation types (up to 0.55 considering PZIN and 0.31 for SPEI-4). The larger absolute values of mean drought tendencies under cyclonic circulation types were compensated by lower frequencies of these types (Figure 3). Positive drought tendencies were found also under the directional circulation types except for the E, SE, and S types (Figure 6). Although a relatively large range between mean drought tendencies in COLD and VEG were found for some circulation types, this range always remained completely within the positive or negative sector (Figure 6). The only exception was the CS circulation type linked to SPEI-4, which had positive mean drought tendency in COLD and slightly negative in VEG.

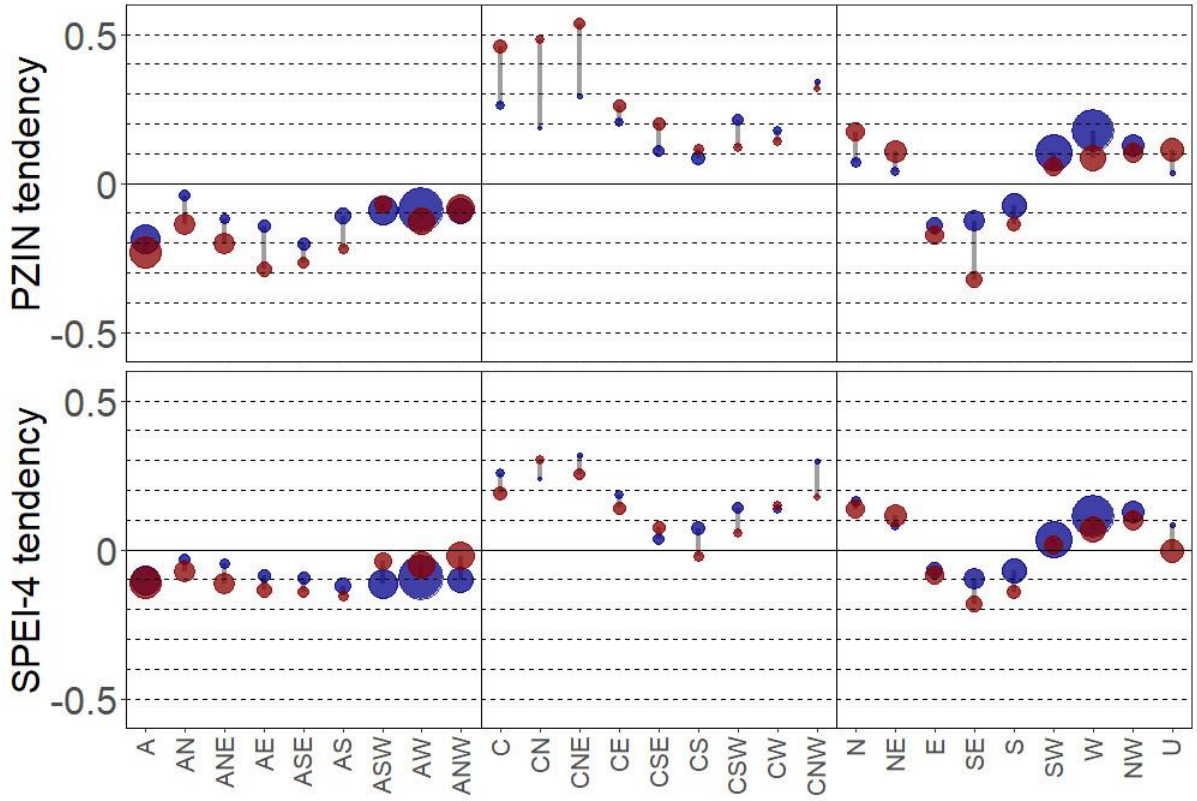

Figure 6. Mean drought tendency for 27 circulation types using two short-term drought indices, PZIN and SPEI-4. Red circles represent the vegetation period, while blue ones stand for the cold period. The size of each circle indicates the given circulation type' frequency of occurrence.

Based on these results, 12 circulation types with negative mean drought tendency (averaged between PZIN and SPEI-4) were defined. Those were all anticyclonic types (A, AN, ANE, AE, ASE, AS, ASW, AW, ANW) and directional types from the southeast quadrant (E, SE, and S; hereafter referred altogether as dry circulation types). The remaining 15 circulation types, i.e. all cyclonic types (C, CN, CNE, CE, CSE, CS, CSW, CW, CNW), directional types with northern and/or western component (NE, N, NW, W, SW), and undefined type (U), had positive mean drought tendencies and were labeled as wet types.

The annual frequency of dry circulation types during VEG had a statistically significant positive trend in the 1948–2018 period (roughly 2%/decade), and its largest value (68%) was found in 2015. During the last 30 years, dry circulation types occurred more frequently compared to wet ones in 23 out of 30 VEG seasons, which is a completely opposite pattern compared to that observed in the 1950s and 1960s (Figure 7a). For COLD, the positive trend of dry circulation types' frequency had smaller magnitude (less than 1% per decade) and was not statistically significant (Figure 7b). The COLD seasons in the 2015–2018 dry period had average or even below-average frequency of dry circulation types compared to other seasons and therefore the 2015–2018 drought probably originated mainly from the dryness during vegetation periods.

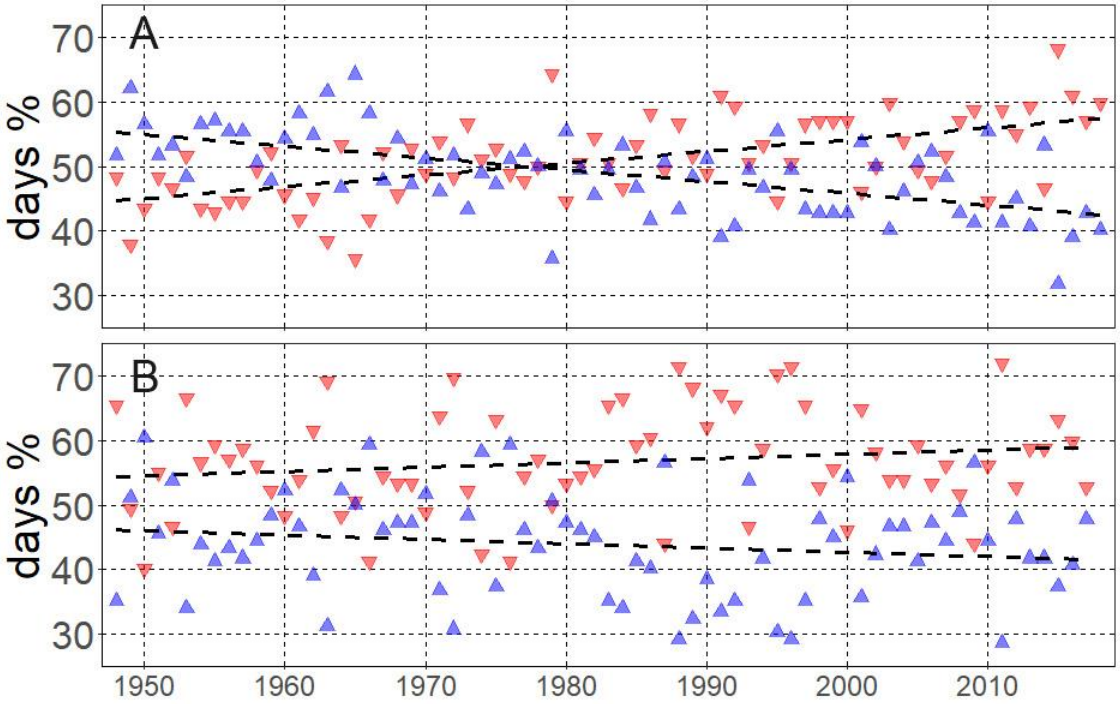

Figure 7. Temporal variability of the frequencies of dry (red) and wet (blue) circulation types with least-square regression lines, for vegetation period (A) and cold period (B).

3.3 Dry period of 2015–2018

In this section, the dry 2015–2018 period is analyzed in more detail using both long-term and short-term indices, averaged over all seven stations. Prevailing wet conditions of 2013, due to floods in Central Europe (Blöschl et al., 2013), were succeeded by transition to a drier regime by the beginning of 2014, as reflected in the long-term indices (PDSI and SPEI-52; Figure 8).

316 The first severe drought episode according to those indices was recorded during mid-2014,
317 followed by moister conditions at the end of the year, partially replenishing water availability
318 before the extreme episode of 2015. The extreme drought that developed in that summer was
319 preceded by an exceptionally high number of dry circulation types. The extreme drought
320 conditions persisted until mid–2016 (according to SPEI-52) or the end of 2016 (considering
321 PDSI). The largest discrepancy between the long-term drought indices was found during 2016–
322 2017, when severe drought persisted according to PDSI, but only a short episode of moderate
323 drought in mid–2017 was found using SPEI-52 (discussed in Section 4). In the first half of 2018,
324 both long-term indices dropped to severe drought level and drought conditions peaked in the
325 second half of the year, associated with a high frequency of dry circulation types, comparable to
326 that observed in the first half of 2015. The PDSI index reached a record-breaking value in 2018,
327 but drought conditions were more extreme in 2015 according to SPEI-52 (Figure 8).
328 Drought episodes had, as expected, shorter duration when analyzed by the short-term
329 indices. There was good agreement between PZIN and SPEI-4 on severe drought episodes and
330 those indices were better linked to circulation types. Within the 2013–2018 period, both PZIN
331 and SPEI-4 showed extreme drought conditions in mid-2015. SPEI-4 indicated considerably
332 more drought events, however, with some extreme events occurring during the beginning of
333 2014 and in mid-2018 (Figure 8).

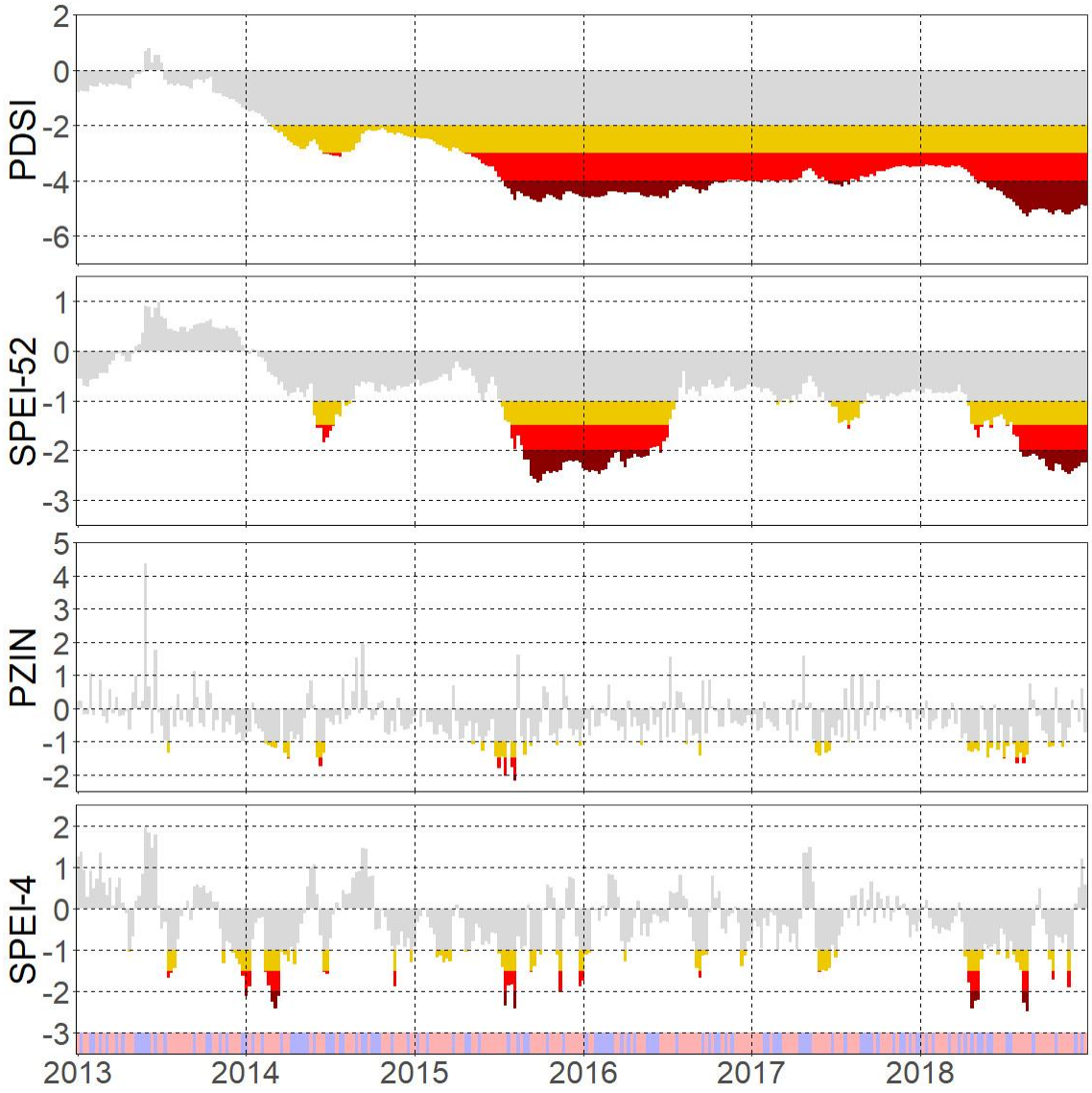

Figure 8. Temporal development of Palmer Drought Severity Index (PDSI), long-term Standardized Precipitation Evaporation Index (SPEI-52), Palmer Z-index (PZIN), and short-term Standardized Precipitation Evaporation Index (SPEI-4) in the 2013–2018 period. Yellow color indicates moderate, red severe, and dark red extreme drought conditions. Red bars represent dry circulation types, while blue ones stand for wet circulation types.

4 Discussion

The analysis demonstrates that the 2015–2018 drought in the Czech Republic was of record-breaking severity on a centennial scale according to various indices. The spatial extent of the event also was uncommon. The extreme drought occurred concurrently at all stations, revealing a characteristic homogeneity that has occurred only once in the whole record. These findings are also supported by empirical studies that confirm positive shifts in summer or annual evapotranspiration in Central and Eastern Europe (Bogawski & Bednorz, 2016; Duethman & Blöschl, 2018; Maček et al., 2018; Prăvălie et al., 2019). This shift in drought conditions is coupled with a monotonous increase in the number of days with dry circulation types in the vegetation period. Similarly, during the 2015–2018 drought, the same dry circulation types dominated the respective vegetation periods.

Initiation of the 2015–2018 drought coincides with the pan-European 2015 drought event (Ionita et al., 2017; Laaha et al., 2017). Although the severity of hydrological drought (streamflow levels) was not very extreme for the larger part of Europe, this was not the case for Central Europe. The main reason was found in the hydrologic preconditions of each catchment (Laaha et al., 2017). According to the local hydrographs, extreme droughts occurred as a consequence of dry preconditions in the preceding winter and/or spring. In those catchments where wet preconditions prevailed, low streamflow events were less severe. Our results support this hypothesis. Dry conditions prevailed at all 7 stations analyzed (Figure 4), and the one with the highest drought intensity in 2015 (Brno) had been experiencing the longest dry period beforehand.

It should be noted that Feng et al. (2017) reported that severity of droughts in warmer climate might be overestimated when estimates of potential evapotranspiration are based on Thornthwaite's temperature-driven approach. Central Europe experienced a rapid increase of summer temperatures recently (Christidis et al., 2015) and use of the Thornthwaite's method might lead to overestimation of the computed exceptional drought severity in 2015–2018 compared to previous episodes. It has to be considered, however, that reliable and consistent data of all input parameters needed for Penman–Monteith formula application are rarely available especially for the period prior to 1900. Therefore the Thornthwaite's method is the only realistic option available for estimating potential evapotranspiration in this study.

In addition, the fingerprints of other significant pan-European drought events are well-represented in our analysis. In 1947, for instance, a well-documented drought had occurred that was followed by other drought events with lower spatial extent, marking a prolonged period of frequent drought events in Europe ending around 1954 (Moravec et al., 2019; Spinoni et al., 2015). The 1947 event is detected in the PDSI of 4 stations (Figure 4), while other consequent events are also evident at different stations, with varying initiations, durations, and terminations. The long-term fingerprint of this period (i.e., 1947–1954) can be seen in Danube streamflow, as its catchment extends over the majority of the affected regions (Pekarova et al., 2006).

The considerable difference in drought severity between PDSI and SPEI-52 from mid-2016 to mid-2018 is primarily caused by the inclusion of available soil water content into PDSI. In contrast to SPEI-52, past precipitation deficit in PDSI therefore propagates into the following weeks until soil moisture recovers to normal values (WMO and GWP, 2016). Thus, PDSI tends to capture groundwater deficits better (which was observed also during 2017; Crhová et al., 2018) while SPEI-52 seems to show more realistic drought conditions in upper soil layers during this period. In terms of drought initiation, SPEI-52 appears to better match the results of Ionita et al. (2017), who detected initiation of the 2015 event in May.

386 The anticyclonic and southeasterly circulation types were identified as conducive to
387 drought and these findings are in accordance with Trnka et al. (2009), who used the subjective
388 Hess–Brezowsky catalogue (Werner and Gerstengarbe, 2009) for the 1881–2005 period. Trnka
389 et al. (2009) found increasing abundance of dry circulation types over Central Europe since the
390 mid-20th century (considering the April–June period). The statistically significant increment in
391 the frequency of dry advection was observed also in our study, using updated data series (up to
392 2018) and objectively classified circulation types. This is also in accordance with Horton et al.
393 (2015), who showed robust positive trends in the occurrence, persistence, and maximum duration
394 of summer anticyclonic patterns over Europe in the 1979–2013 period.
395 The increase of anticyclonic patterns (dry circulation types) in the vegetation period has a
396 pronounced effect in drought propagation. Inasmuch as these patterns are related to both lower
397 precipitation and higher temperatures, they accelerate soil moisture depletion. This can produce a
398 positive feedback mechanism between soil moisture and climate (Seneviratne et al., 2006). A
399 decline in soil moisture affects the stability of the boundary layer and reduces the frontal
400 systems' ability to precipitate, which can exacerbate the duration and intensity of drought events.
401 In addition, evapotranspiration is directly linked with soil moisture, which in turn impacts the
402 flux of sensible heat and thus air temperature. A decrease in evapotranspiration means that air
403 closer to the ground needs a higher amount of time to cool. This is a plausible hypothesis for the
404 link between low precipitation, increased evaporative demand, and the extremity of recent
405 drought during the vegetation period that has been reported to be extremely severe in a 250-year
406 time window (Hanel et al., 2018).
407 The persistent circulation patterns are often linked to upper-tropospheric Rossby wave–
408 like structures (Schubert et al., 2011), which are associated with hot and dry summers over
409 Eurasia (Röthlisberger et al., 2016). Relationships between characteristics of Rossby waves (e.g.,
410 their amplitude or propagation) and large-scale forcing have been widely discussed, with a view
411 to rapid climate change in the Arctic (Cohen et al., 2014; Francis et al., 2017), temperature
412 characteristics of the Atlantic Ocean (Duchez et al., 2016; Sutton & Dong 2012) or the role of
413 the El-Nino Southern Oscillation (Kang et al., 2014). This variety of interconnected factors
414 makes modeling of atmospheric circulation challenging, creating relatively large uncertainties in
415 future weather and climate extremes, including severe droughts (Woolings, 2010).
416 In the future climate, in general, the hydrological cycle is projected to become more
417 intense in the warmer atmosphere, potentially resulting in increased frequency of droughts (Dai
418 & Zhao 2017; Prudhomme et al., 2014). On the European scale, the largest increment of drought
419 severity is projected over the Mediterranean due to a combination of lower precipitation and
420 higher temperatures (Spinoni et al., 2018). By contrast, modeled changes of drought severity
421 over Central Europe are not statistically significant, mainly due to the simulated increase in
422 precipitation (Jacob et al., 2014). The negative trends in drought indices presented in our study
423 contradict this hypothesis. Our results support the argument that it remains challenging for
424 current climate models to sufficiently simulate changes in atmospheric circulation, which can
425 propagate into precipitation biases (Kotlarski et al., 2014). Other reported issues involve the lack
426 of a robust framework for the representation of cloud microphysics that create precipitation
427 (Sherwood et al., 2010), significant biases in reproducing rainfall intermittency (Trenberth et al.,
428 2017), and the simplified representation of land–atmosphere feedbacks (Miralles et al., 2019)
429 that can substantially intensify heat waves and droughts (Teuling, 2018).

5 Conclusions

Using four drought indices calculated at 7 stations with long-term records in the Czech Republic, we studied long-term variability of droughts and their links to atmospheric circulation, with focus on the recent 2015–2018 dry period. The main findings are as follow:

- Severity of the 2015–2018 dry period was record-breaking, especially when considering the long-term drought indices. PDSI values below –6 were recorded in Brno and Prague during this period, and that was unprecedented in the centennial instrumental records.

- The dry 2015–2018 period contributed to statistically significant PDSI trends toward drier conditions over the 1922–2018 period. Analogous results were obtained for the other long-term index, SPEI-52.

- Short-term drought indices (PZIN and SPEI-4) showed more pronounced negative trends in the vegetation period compared to the cold period, suggesting that the dryness of 2015–2018 originated mainly from droughts in the warm halves of the given years. The two lowest PZIN values for vegetation period were recorded in 2015 and 2018, and similar results were found for SPEI-4.

- Frequency of dry (wet) circulation types exhibited a statistically significant positive (negative) trend for the vegetation period over 1948–2018, and this trend contributed to the observed increasing drought frequency and severity. Similar but insignificant trends in dry and wet circulation types were found also for the cold period.

- The drought in vegetation periods during 2015–2018 was associated with above-average frequencies of dry circulation types and decline in wet ones. The record-high seasonal abundance of dry circulation types was found in the vegetation period of 2015.

The last point highlights the strong relationship between major droughts and atmospheric circulation, implying that construction of future drought scenarios should be preceded by thorough evaluation of climate models' simulations for the recent climate, with a focus on their ability to represent observed changes in atmospheric circulation and their links to surface meteorological variables. It remains an open question, however, whether the unusually large number of dry years in the past decade is driven by climate change or whether it is a part of natural variability of Central European climate.

Acknowledgments, Samples, and Data

OL's contribution was carried within the INTER-COST project funded by the Ministry of Education, Youth and Sports of the Czech Republic (project no. LTC19044). JK and YM were supported by "XEROS: eXtremeEuRopeandrOughtS: Multimodel synthesis of past, present and future events," a bilateral project of the Czech Science Foundation (grant no. 19-24089J) and the Deutsche Forschungsgemeinschaft (grant RA 3235/1-1). MT, JB, and MM were supported by project "SustES - Adaptation strategies for sustainable ecosystem services and food security under adverse environmental conditions" (CZ.02.1.01/0.0/0.0/16_019/0000797).

We acknowledge the NCEP Reanalysis data provided by the NOAA/OAR/ESRL PSD, Boulder, Colorado, USA, which can be obtained from https://www.esrl.noaa.gov/psd/data/gridded/data.ncep.reanalysis.html. Drought indices calculated for this study are available on following data repository: https://data.mendeley.com/datasets/7rfdm4bg9g/draft?a=5454df40-acba-4e04-ad7e-b094e025c330.

References

Allen, R. G. L., Pereira, S., Raes, D., & Smith, M. (1998). *Crop evapotranspiration: Guidelines for computing crop water requirements.* FAO Report 56, 300 pp. Retrieved from http://www.fao.org/docrep/X0490E/X0490E00.htm

Brázdil, R., Trnka, M., Mikšovský, J., Řezníčková, L., & Dobrovolný, P. (2015). Spring−summer droughts in the Czech Land in 1805–2012 and their forcings. *International Journal of Climatology, 35,* 1405–1421. http://doi.org/10.1002/joc.4065

Blöschl, G., Nester, T., Komma, J., Parajka, J., & Perdigao, R. A. P. (2013). The June 2013 flood in the Upper Danube Basin, and comparisons with the 2002, 1954 and 1899 floods. *Hydrology and Earth System Sciences, 17,* 5197–5212. http://doi.org/10.5194/hess-17-5197-2013

Bogawski, P., & Bednorz, E. (2016). Atmospheric conditions controlling extreme summertime evapotranspiration in Poland (central Europe). *Natural Hazards, 81,* 55–69. http://doi.org/10.1007/s11069-015-2066-2

Christidis, N., Jones, G. S., & Stott, P. A. (2015). Dramatically increasing chance of extremely hot summers since the 2003 European heatwave. *Nature Climate Change, 5*, 46–50. http://doi.org/10.1038/nclimate2468

Cohen, J., Screen, J. A. , Furtado, J. C., Barlov, M., Whittleston, D., Coumou, D., et al. (2014). Recent Arctic amplification and extreme mid-latitude weather. *Nature Geoscience, 7,* 627–637. http://doi.org/10.1038/ngeo2234

Collins, M., Knutti, R., Arblaster, J., Dufresne, J-L., Fichefet, T., Friedlingstein, P., et al. (2013). Near-term Climate Change: Projections and Predictability. In: *Climate Change 2013: The Physical Science Basis. Contribution of Working Group I to the Fifth Assessment Report of the Intergovernmental Panel on Climate Change.* Cambridge University Press, Cambridge, United Kingdom and New York, NY, USA

Crhová, L., Čekal, R., & Černá, L. (2018). *Roční zpráva o hydrometeorologické situaci v České republice 2017* [in Czech]. Czech Hydrometeorological Institute. Retrieved from http://portal.chmi.cz/files/portal/docs/hydro/sucho/Zpravy/ROK_2017.pdf

Dai, A. (2011). Characteristics and trends in various forms of the Palmer Drought Severity Index during 1900–2008. *Journal of Geophysical Research, 116,* D12115. http://doi.org/10.1029/2010JD015541

Dai, A., & Zhao, T. (2017). Uncertainties in historical changes and future projections of drought. Part I: estimates of historical drought changes. *Climatic Change, 144,* 519–533. http://doi.org/10.1007/s10584-016-1705-2

Delworth, T. L., & Manabe, S. (1988). The influence of potential evaporation on the variabilities of simulated soil wetness and climate. *Journal of Climate, 1,* 523-547.

Duchez, A., Frajka-Williams, E., Josey, S. A., Evans, D. G., Grist, J. P., Marsh, R., et al. (2016). Drivers of exceptionally cold North Atlantic Ocean temperatures and their link to the 2015 European heat wave. *Environmental Research Letters, 11,* 074004. http://doi.org/10.1088/1748-9326/11/7/074004

European Commision (EC) (2018). *Report: EU agricultural markets short-term outlook - Autumn 2018.* Retrieved from https://ec.europa.eu/info/files/report-eu-agricultural-markets-short-term-outlook-autumn-2018_en

Feng, S., Trnka, M., Hayes, M., Zhang, Y. (2017). Why Do Different Drought Indices Show Distinct Future Drought Risk Outcomes in the U.S. Great Plains? *Journal of Climate, 30,* 265–278. http://doi.org/10.1175/JCLI-D-15-0590.1

Fischer, E. M., & Schär, C. (2010). Consistent geographical patterns of changes in high-impact European heatwaves. *Nature Geoscience, 3,* 398–403. http://doi.org/10.1038/ngeo866

Francis, J. A., Vavrus, S. J., Cohen, J. (2017). Amplified Arctic warming and mid-latitude weather: new perspectives on emerging connections. *Wiley Interdisciplinary Reviews: Climate Change, 8,* 1–11. http://doi.org/10.1002/wcc.474

Guttman, N. B. (1998). Comparing the Palmer Drought Index and the Standardized Precipitation Index. *Journal of the American Water Resources Association, 34,* 113–121, http://doi.org/10.1111/j.1752-1688.1998.tb05964

Hanel, M., Rakovec, O., Markonis, Y., Máca, P., Samaniego, L., Kyselý, J., & Kumar, R. (2018). Revisiting the recent European droughts from a long-term perspective. *Scientific Reports, 8,* 9499. http://doi.org/10.1038/s41598-018-27464-4

Hartmann, D. L, Klein Tank, A. M. G., Rusticucci, M., Alexander, L. V., Brönnimanm, S., Charabi J. A-R., et al. (2013). Observations: Atmosphere and Surface. In: *Climate Change 2013: The Physical Science Basis. Contribution of Working Group I to the Fifth Assessment Report of the Intergovernmental Panel on Climate Change.* Cambridge University Press, Cambridge, United Kingdom and New York, NY, USA

Hayes, M., Svoboda, M., Wall, N., & Widhalm, M. (2011). The Lincoln Declaration on Drought Indices: Universal Meteorological Drought Index Recommended. *Bulletin of the American Meteorological Society, 92,* 485–488. http://doi.org/10.1175/2010bams3103.1

Heim, R.R. (2002). A Review Century Drought of Twentieth - the United States Indices Used. *Bulletin of the American Meteorological Society, 83,* 1149–1165.

Horton, D. E., Johnson, N. C., Singh, D., Swain, D. L., Rajaratnam, B., & Diffenbaugh, N. S. (2015). Contribution of changes in atmospheric circulation patterns to extreme temperature trends. *Nature, 522,* 465–469. http://doi.org/10.1038/nature14550

Hoy, A., Hänsel, S., Skalak, P., Ustrnul, Z., & Bochníček, O. (2017). The extreme European summer of 2015 in a long-term perspective. *International Journal of Climatology, 37,* 943–962. http://doi.org/10.1002/joc.4751

Ionita, M., Tallaksen, L. M., Kingston, D. G., Stagge, J. H., Laaha, G., Van Lanen, H. A. J., et al. (2017). The European 2015 drought from a climatological perspective. *Hydrology and Earth System Sciences, 21,* 1397–1419. http://doi.org/10.5194/hess-21-1397-2017

Jacob, D., Petersen, J., Eggert, B., Alias, A., Christensen, O.B., Bouwer, L.M., et al. (2014). EURO-CORDEX: new high-resolution climate change projections for European impact research. *Regional Environmental Change,* 14, 563–578. https://doi.org/10.1007/s10113-013-0499-2

Jenkinson, A. F., & Collison, F. P. (1977). An initial climatology of gales over the North Sea, *Synoptic Climatology Branch Memorandum* No. 62, Meteorological Office, Bracknell, United Kingdom

Kalnay, E., Kanamitsu, M., Kistler, R., Collins, W., Deaven, D., Gandin, L., et al. (1996). The NCEP/NCAR 40-year reanalysis project. *Bulletin of the American Meteorological Society, 77,* 437–471.

Kang, I-S., No, H-H., & Kucharski, F. (2014). ENSO Amplitude Modulation Associated with the Mean SST Changes in the Tropical Central Pacific Induced by Atlantic Multidecadal Oscillation. *Journal of Climate, 27,* 7911–7920. https://doi.org/10.1175/JCLI-D-14-00018.1

Kotlarski, S., Keuler, K., Christensen, O.B., Collete, A., Déqué, M., Gobiet, A., et al. (2014). Regional climate modeling on European scales: A joint standard evaluation of the EURO-CORDEX RCM ensemble. *Geoscientific Model Development,* 7, 1297–1333. https://doi.org/10.5194/gmd-7-1297-2014

Laaha, G., Gauster, T., Tallaksen, L. M., Vidal, J. P., Stahl, K., Prudhomme, C., et al. (2017). The European 2015 drought from a hydrological perspective. *Hydrology and Earth System Sciences, 21,* 3001–3024. https://doi.org/10.5194/hess-21-3001-2017

Lhotka, O., Kyselý, J., & Farda, A. (2018a). Climate change scenarios of heat waves in Central Europe and their uncertainties. *Theoretical and Applied Climatology, 131,* 1043–1054. https://doi.org/10.1007/s00704-016-2031-3

Lhotka, O., Kyselý, J., & Plavcová, E. (2018b). Evaluation of major heat waves' mechanisms in EURO-CORDEX RCMs over Central Europe. *Climate Dynamics, 50,* 4249–4262. https://doi.org/10.1007/s00382-017-3873-9

Maček, U., Bezak, N., & Šraj, M. (2018). Reference evapotranspiration changes in Slovenia, Europe. *Agricultural and Forest Meteorology, 260,* 183–192. http://doi.org/10.1016/j.agrformet.2018.06.014

Markonis, Y., Hanel, M., Máca, P., Kyselý, J., & Cook, E. R. (2018). Persistent multi-scale fluctuations shift European hydroclimate to its millennial boundaries. *Nature Communications, 9,* 1–12. http://doi.org/10.1038/s41467-018-04207-7

Miralles, D. G., Gentine, P., Seneviratne, S. I., & Teuling, A. J. (2019). Land-atmospheric feedbacks during droughts and heatwaves: state of the science and current challenges. *Annals of the New York Academy of Sciences, 1436,* 19–35. http://doi.org/10.1111/nyas.13912

Miralles, D. G., Teuling, A. J., Van Heerwaarden, C. C., & Vilà-Guerau de Arellano, J. (2014). Mega-heatwave temperatures due to combined soil desiccation and atmospheric heat accumulation. *Nature Geoscience, 7,* 345–349. http://doi.org/10.1038/ngeo2141

Moravec, V., Markonis, Y., Rakovec, O., Kumar, R., & Hanel, M. (2019). A 250-year European drought inventory derived from ensemble hydrologic modelling. *Geophysical Research Letters, 46,* 5909–5917. https://doi.org/10.1029/2019GL082783

Palmer, W. C. (1965). Meteorological Drought. Research Paper No. 45, US Weather Bureau, Washington, DC

Pekarova, P., Miklanek, P., Pekar, J. (2006). *Long-term trends and runoff fluctuations of European rivers.* IAHS Publ. 308, 520–525. Retrieved from https://iahs.info/uploads/dms/13714.94-520-525-97-308-Pekarova.pdf

Plavcová, E., & Kyselý, J. (2011). Evaluation of daily temperatures in Central Europe and their links to large-scale circulation in an ensemble of regional climate models. *Tellus A, 63A,* 763–781. http://doi.org/10.1111/j.1600-0870.2011.00514.x

Prăvălie, R., Piticar, A., Roșca, B., Sfîcă, L., Bandoc, G., Tiscovschi, A., & Patriche, C. (2019). Spatio-temporal changes of the climatic water balance in Romania as a response to precipitation and reference evapotranspiration trends during 1961–2013. *Catena,* 17, 295–312. http://doi.org/10.1016/j.catena.2018.08.028

Prudhomme, C., Giuntoli, I., Robinson, E. L., Clark, D. B., Arnell, N. W., Dankers, R., et al. (2014). Hydrological droughts in the 21st century, hotspots and uncertainties from a global multimodel ensemble experiment. *Proceedings of the National Academy of Sciences, 111,* 3262–3267. http://doi.org10.1073/pnas.1222473110

Röthlisberger, M., Pfahl, S., & Martius, O. (2016). Regional - scale jet waviness modulates the occurrence of midlatitude weather extremes. *Geophysical Research Letters 43,* 10 989–10 997. http://doi.org/10.1002/2016GL070944.

Schubert, S., Wang, H., & Suarez, M. (2011). Warm Season Subseasonal Variability and Climate Extremes in the Northern Hemisphere: The Role of Stationary Rossby Waves. *Journal of Climate, 24,* 4773–4792 . http://doi.org/10.1175/JCLI-D-10-05035.1

Seneviratne, S.I., Lüthi, D., Litschi, D., & Schär, C. (2006). Land–atmosphere coupling and climate change in Europe. *Nature, 443,* 205–209. http://doi.org/10.1038/nature05095

Sheffield, J., Wood, E. F., & Roderick, M. L. (2012). Little change in global drought over the past 60 years. *Nature, 491,* 435–438 http://doi.org/10.1038/nature11575

Sherwood, S. C., Roca, R., Weckwerth, T. M., & Andronova, N. G. (2010). Tropospheric water vapor, convection, and climate. *Review Geophysics, 48,* RG2001. http://doi.org/10.1029/2009RG000301.

Spinoni, J., Naumann, G., & Vogt, J. V. (2017). Pan-European seasonal trends and recent changes of drought frequency and severity. *Global Planetary Change, 148,* 113–130. http://doi.org/10.1016/j.gloplacha.2016.11.013

Spinoni, J., Naumann, G., Vogt, J. V., & Barbosa, P. (2015). The biggest drought events in Europe from 1950 to 2012. *Journal of Hydrology: Regional Studies, 3,* 509–524. http://doi.org/10.1016/j.ejrh.2015.01.001.

Spinoni, J., Vogt, J. V., Naumann, G., Barbosa, P., & Dosio, A. (2018). Will drought events become more frequent and severe in Europe? *International Journal of Climatology, 38,* 1718–1736. http://doi.org/10.1002/joc.5291

Stéfanon, M., Drobinski, P., D'Andrea, F., & Brossier, C. L. (2014). Soil moisture-temperature feedbacks at meso-scale during summer heat waves over Western Europe. *Climate Dynamics, 42,* 1309–1324. http://doi.org/10.1007/s00382-013-1794-9

Sutton, R. T., & Dong, B. (2012). Atlantic Ocean influence on a shift in European climate in the 1990s. *Nature Geoscience, 5,* 788–792. http://doi.org/10.1038/ngeo1595

Teuling, A. J. (2018). A hot future for European droughts. *Nature Climate Change, 8,* 364–365. http://doi.org/10.1038/s41558-018-0154-5

Thornthwaite, C. W. (1948). Anapproach toward a rational classification of climate. *Geographical Review, 38,* 55–94. http://doi.org/10.2307/210739

Trenberth, K. E., Zhang, Y., & Gehne, M. (2017). Intermittency in Precipitation: Duration, Frequency, Intensity, and Amounts Using Hourly Data. *Journal of Hydrometeorology, 18,* 1393–1412. http://doi.org/10.1175/JHM-D-16-0263.1

Trnka, M., Brázdil, R., Možný, M., Štěpánek, P., Dobrovolný, P., Zahradníček, P., et al. (2015). Soil moisture trends in the Czech Republic between 1961 and 2012. *International Journal of Climatology, 35,* 3733–3747. http://doi.org/10.1002/joc.4242

Trnka, M., Feng, S., Semenov, M. A. , Olesen J. E., Kersebaum, K. C., Rötter, R. P., et al (2019). Mitigation efforts will not fully alleviate the increase in water scarcity occurrence probability in wheat-producing areas. *Science Advances, 5,* eaau2406. http://doi.org/10.1126/sciadv.aau2406

Trnka, M., Kyselý, J., Možný, M., & Dubrovský, M. (2009). Changes in Central-European soil-moisture availability and circulation patterns in 1881-2005. International Journal of Climatology 29, 655–672. http://doi.org/10.1002/joc.1703

Vicente-Serrano, S. M., Begueria, S., & Lopez-Moreno, J.I. (2010). A multi-scalar drought index sensitive to global warming: the Standardized Precipitation Evapotranspiration Index. *Journal of Climate, 23,* 1696–1718. http://doi.org/10.1175/2009JCLI2909.1

Vicente-Serrano, S. M., Lopez-Moreno, J-I., Beguería, S., Lorenzo-Lacruz, J., Sanchez-Lorenzo, A., García-Ruiz, J. M., et al. (2015). Evidence of increasing drought severity caused by temperature rise in southern Europe. *Environmental Research Letters, 9,* 044001. http://doi.org/ 10.1088/1748-9326/9/4/044001

Werner, P. C., & Gerstengarbe, F. V. (2009). *Katalog der grosswetterlagen Europas (1881-2009).* Potsdam Institute for Climate Impact Research

Woolings, T. (2010). Dynamical influences on European climate: an uncertain future. *Philosophical Transactions of the Royal Society A: Mathematical, Physical and Engineering Sciences, 368,* 3733–3756. http://doi.org/10.1098/rsta.2010.0040

World Meteorological Organization (WMO) and Global Water Partnership (GWP) (2016). *Handbook of Drought Indicators and Indices.* Geneva. ISBN: 978-92-63-11173-9

671 United Nations (UN) (2018). Drought and conflict leave millions more hungry in 2017 – UN –
672 backed report. Retrieved from https://news.un.org/en/story/2018/03/1005621

673 Yue, S., & Wang, C. Y. (2004). The Mann-Kendall test modified by effective sample size to
674 detect trend in serially correlated hydrological series. *Water Resources Management, 18,*
675 201–218. http://doi.org/10.1023/B:WARM.0000043140.61082.60